Journal Pre-proofs

Original Article

Potential and pitfalls of 1.5 T MRI imaging for target volume definition in ocular proton therapy

Riccardo Via, Fabian Hennings, Alessia Pica, Giovanni Fattori, Jürgen Beer, Marta Peroni, Guido Baroni, Antony Lomax, Damien Charles Weber, Jan Hrbacek

Please cite this article as: Via, R., Hennings, F., Pica, A., Fattori, G., Beer, J., Peroni, M., Baroni, G., Lomax, A., Charles Weber, D., Hrbacek, J., Potential and pitfalls of 1.5 T MRI imaging for target volume definition in ocular proton therapy, *Radiotherapy and Oncology* (2020), doi: https://doi.org/10.1016/j.radonc.2020.08.023
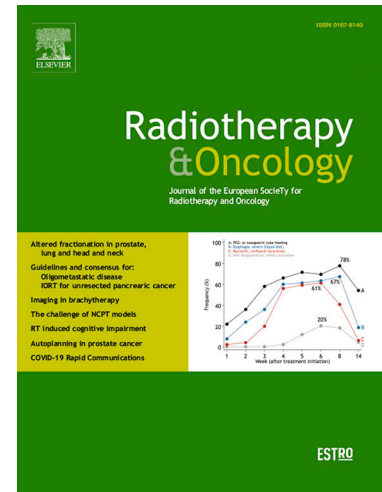
Title:

Potential and pitfalls of 1.5 T MRI imaging for target volume definition in ocular proton therapy

Short title:

1.5 T MRI eye modelling in ocular proton therapy

Authors (Name and Surname)

Riccardo Via PhD [1], Fabian Hennings PhD [1], Alessia Pica MD [1], Giovanni Fattori PhD [1], Jürgen Beer MD[1], Marta Peroni PhD [1], Guido Baroni PhD [4], Antony Lomax PhD [1], Damien Charles Weber MD [1,2,3], Jan Hrbacek PhD [1]

Affiliations:

[1] Paul Scherrer Institut (PSI), Center for Proton Therapy, 5232 Villigen PSI, Switzerland
[2] Department of Radiation Oncology, University Hospital Zurich, Rämistrasse 100, 8091 Zurich, Switzerland
[3] Department of Radiation Oncology, University Hospital Bern, Freiburgstrasse 18, 3010 Bern Switzerland
[4] Dipartimento di Elettronica Informazione e Bioingegneria, Politecnico di Milano, Milano 20133, Italy

Corresponding author:

Riccardo Via, PhD
Mailing address: WMSA/C29, 5232 Villigen PSI, Switzerland
e-mail: riccardo.via@psi.ch
Phone: +41 56 310 54 05

Potential and pitfalls of 1.5T MRI imaging for target volume definition in ocular proton therapy

ABSTRACT

Introduction: Ocular proton therapy (OPT) for the treatment of uveal melanoma has a long and remarkably successful history. This is despite that, for the majority of patients treated, the definition of the eye anatomy is based on a simplified geometrical model embedded in the treatment planning system EyePlan. In this study, differences in anatomical and tumor structures from EyePlan, and those based on 1.5T magnetic resonance imaging (MRI) are assessed.

Materials and Methods: Thirty-three uveal melanoma patients treated with OPT at our institution were subject to eye MRI. The target volumes were manually delineated on those images by two radiation oncologists. The resulting volumes were geometrically compared to the clinical standard. In addition, the dosimetric impact of using different models for treatment planning were evaluated.

Results: Two patients (6%) presented lesions too small to be visible on MRI. Target volumes identified on MRI scans were on average smaller than EyePlan with discrepancies arising mostly from the definition of the tumor base. Clip-to-tumor base distances measured on MRI models exhibited higher discrepancy to ophthalmological measurements than EyePlan. For 53% of cases, treatment plans optimized for lesions identified on MRI only, failed to achieve sufficient target coverage for EyePlan volumes.

Discussion: The analysis has shown that 1.5T MRI might be more susceptible to misses of flat tumor extension of the clinical target volume than the current clinical standard. Thus, a proper integration of ancillary imaging modalities, leading to a better characterization of the full lesion, is required.

INTRODUCTION

The treatment of uveal melanoma with proton therapy has a long and successful history, with more than 30'000 patients having been treated worldwide, achieving tumor control rates at 5 years of well over 90% [1] [2] [3]. Of these, more than 20% of all such treatments have been delivered at Paul Scherrer Institut (PSI), with tumor control rates reaching 98% [4] [5].

The current treatment procedure relies on a geometrical model of the eye and tumor, generated in the EyePlan treatment planning system [1] [6] [2], fitted to fiducial markers (tantalum clips) sutured on the sclera during a surgical intervention. While other imaging modalities (e.g. ultrasonography, fundus etc.) are taken into consideration when generating the model, it is the marker positions, derived from orthogonal x-ray imaging, that provide the geometrical reference for target volume definition and patient positioning during treatment.

This model is unquestionably a simplification and neglects individual patient specificity when defining organs at risk. However, using fiducials as close as possible to the target ensures high accuracy for tumor localization, and its validity is confirmed by the high tumor control rates achieved across all centers. On the other hand, tumor control has also been shown to be very sensitive to even small modifications to the target volume [4].

A recent clinical survey indicated that there is an increased interest in bringing three-dimensional imaging modalities (computed tomography- CT/ Magnetic Resonance Imaging-MRI) into the clinic as a means of validation or to enhance the geometrical model of the eye [1]. At the Helmholtz-Zentrum Berlin für Materialien und Energie (HZB) in Berlin, for example, volumetric eye imaging has been integrated in their in-house treatment planning system (TPS; OCTOPUS) [7] [8] [9] [10]. Slopsema et al. also argue for using CT imaging to improve the geometrical eye model and Marnitz et al. [11] report reductions of target volumes by close to two when comparing fiducial based definition to delineation in MRI scans [3]. In contrast, Daftari et al [9] found more similar volume ratios of between

0.993 and 1.02 for delineations using EyePlan or T2-weighted MRI imaging [12]. Such ambiguous results suggest that introducing new imaging methods in OPT is not straightforward and should be pursued cautiously.

In this study we investigate the potential and limitations of MRI for modelling of the eye and tumor under the hypothesis that MRI will be an essential part of any workflow aiming to replace the use of clips for the definition of the target volume [6] [13]. As such, MRI-based modelling is here compared to that of EyePlan for 33 patients. In contrast to previous publications [3] [12], an extensive description of discrepancies between the different modelling of the target volumes, together with a thorough investigation of the causes, is performed, as well as a study of the potential dosimetric consequences.

METHODS

Patient cohort

Thirty-three patients referred to our institute for OPT were included in this study with a mean age of 57 years (range, 26-81). Six patients (18%) presented with lesions extending in the anterior segment of the eye. In the other 27 cases (82%), the tumor was located proximally or posteriorly to the eye equator. All patients underwent clip surgery and conventional treatment planning in EyePlan, where a geometrical eye globe model (EG_{EP}) and target volume (TV_{EP}) were defined (Figure 1-a). All patients also underwent an Institutional Review Board (EKNZ 2014-217) approved MRI, from which three-dimensional, MRI based descriptions of the eye anatomy (EG_{MR}) and the lesion (TV_{MR}) were additionally defined (Figure 1-b).

Conventional eye model

The EyePlan model defines the eye globe as a geometrical ellipsoid or sphere, adapted to the patient's eye length measured using ultrasound. As part of this model, several critical organs, such as the macula, optic disk and lens, are also defined, whose positions and shape are predefined according to a standardized, generic eye model. For the tumor, the base is first drawn on an unfolded plane representing the posterior surface of the eye (the 'fundus-plane') and defined with respect to the tantalum clips using the clip-to-tumor distances derived during surgery. These are measured using calipers, on the tumor shadow projected onto the exterior surface of the eye using trans-illumination. In addition, fundus photography can provide an additional source of information whereby ocular landmarks, such as the macula and optic disk are registered to the unfolded eye model, allowing for further personalization of the tumor base definition [7] [14]. Finally, tumor height and apex position within the base outline are retrieved from A-mode ultrasound measurements. EyePlan then calculates different geometrical models each enveloping the tumor apex and base, and select the best-fit model to the patient anatomy [6].

EyePlan treatment plans for the 33 cases were calculated as above, and were subject to evaluation and acceptance by the referring ophthalmologist and responsible radiation oncologist.

MRI eye model

MRI images were acquired on a 1.5T MAGNETOM AERA (Siemens, Erlangen, Germany) using a surface loop (diameter: 7cm) and half-head coils. Imaging included 3D volumetric T1-weighted (Interpolated Breath-hold Examination -VIBE) without use of contrast agent and 3D T2-weighted *SPACE (turbo spin echo) sequences with an isotropic resolution of 0.5 mm [15] (Figure 2-a/b, respectively). During image acquisition, patients were asked to

maintain a stable gaze direction by gazing at a fixed point on a mirror placed in front of the patient (Figure 2-c). A description of the sequences used can be found in Table 1.

Rigid image registration and structure segmentation were performed using Velocity (Varian Medical System, Palo Alto, CA, USA). Firstly, T1w and T2w images were rigidly aligned using the lens (high signal uniform region on T1w) as a surrogate for fine correction of residual rotational discrepancies. Next, the external eye surface was delineated on the T1w images by inclusion of the vitreous body (high signal uniform region), anterior chamber, lesion, sclera and cornea resulting in the complete eye globe volume (EG_{MR}).

Tumor delineation however, requires a more thorough integration of T1w and T2w scans. The target volume (TV_{MR}) delineation was performed on all three principal planes (coronal, axial and sagittal) and continuously crosschecked between the registered T1w and T2w scans. Of note, uveal melanomas are identifiable as high signal masses on T1w and as low on T2w scans. In contrast, retinal detachment appears as a moderately high signal region on both T1w and T2w scans, thus allowing to discriminate between tumor and retinal detachment using T2w scans. Finally, the tantalum clips, as delineated on T1w images, completed the MRI model. Note, although not providing a signal, tantalum clips are compatible with MRI and can be delineated by their lack of signal [16].

One radiation oncologist (RO) performed delineation of the eye globe and clips, whereas two independent RO performed tumor contouring.

Geometrical Comparison

The two eye models were first aligned using geometrical references provided by the tantalum clips. For this purpose, least-squares optimized point-based rigid registration between the clip configurations in EG_{EP} and EG_{MR} was applied (Figure 1-c), thus compensating for any change in ocular torsion that occurred between x-ray imaging and MRI acquisition. To evaluate the accuracy of definition on MRI images, and the associated geometrical uncertainties, the differences between inter-clip distances of EyePlan and MRI models were quantified for all patients. In addition, both models were compared by visual inspection of their overlap (Figure 1-c) and more quantitatively using Dice Similarity Coefficient (DSC), the volume ratio (VR) and, for the lesion, the ratio of the base-area (AR).

$$DSC = \frac{2*(V_{MR} \cap V_{EP})}{V_{MR} + V_{EP}} \qquad VR = \frac{V_{MR}}{V_{EP}} \qquad AR = \frac{A_{MR}}{A_{EP}}$$

where V_{EP}, V_{MR} are the volumes of structures delineated in EyePlan and from MRI respectively, and A_{EP}, A_{MR} are the EyePlan/MRI base areas of the lesion. The target contours delineated by both RO on MRI images were independently compared with the EyePlan model and differences in tumor height (TV_h) between the models quantified by approximating tumor volume as a hemi-ellipsoid with a circular base-area equal to the lesion base (TV_A) (see Figure 1-d):

$$V_{hemi-ellipsoid} = \frac{2}{3}*\pi*TV_r^2*TV_h = \frac{2}{3}*TV_A*TV_h \qquad TV_h = \frac{3}{2}*\frac{TV}{TV_A}$$

with TV_r being the radius of the circular base-area TV_A. Finally, all three definitions of the target volumes (Eyeplan, RO1 and RO2) were compared in terms of tumor-to-clip distance against the ophthalmological measurements.

Using the Shapiro-Wilks test, a non-normal data distribution was found and non-parametric statistics therefore used. Volume, area and height differences of each lesion were

compared using Friedman's test and Wilcoxon signed-rank test. Spearman's test was used to evaluate the correlation between lesion area/height and the overall volume.

Dosimetric evaluation

Dose calculations were performed using our in-house dose calculation engine that has been previously validated against the Eye-plan calculation [13], and the V95 to the target (the volume covered by 95% of the prescribed dose) used as a metric for plan quality, with V95 = 100% defined as the requirement for a clinically acceptable plan. To evaluate the dosimetric implications of adopting different ocular anatomy models, two studies were performed:

- The treatment plan created for EG_{EP} and TV_{EP} was applied to EG_{MR} to evaluate the coverage achieved on TV_{EP} and quantify the uncertainties related to differences in the overall eye shape alone. Then, the EyePlan plan was applied on the MRI model and dose coverage of TV_{MR} evaluated.
- A new treatment plan, with the dose distribution optimized on TV_{MR} was generated, and the coverage of TV_{EP} assessed. The dose distribution on TV_{EP} was also evaluated by doubling the component of the margin accounting for clinical uncertainties, according to [17], resulting in a total of 4 mm instead of 2.5 mm. This was applied isotropically to the MRI-defined target.

RESULTS

In two (6%) of thirty-three cases, the tumor was invisible on MRI and were therefore excluded from this analysis.

Mean discrepancies of 0.15 mm ± 0.39 mm were observed for inter-clip distances measured on the EyePlan and MRI models highlighting good geometrical consistency between X-ray and MRI measurement.

The patient cohort exhibited eye globe volumes based on EyePlan and MRI agreeing well, with median ratios of 0.98 (IQR:0.12) and DSC of 0.92 (IQR: 0.03). On the other hand median volumes and base-areas for the lesion were 748 mm^3 (IQR: 1088 mm^3) and 221 mm^2 (IQR: 176 mm^2), respectively using EyePlan. As regards MRI delineation, the median volumes and area of the base of TV_{MR} were 514 mm^3 (IQR: 913 mm^3), 349 mm^3 (IQR: 778 mm^3) and 158 mm^2 (IQR: 165 mm^2), 121 mm^2 (IQR: 139 mm^2) for the two RO respectively.

Target volumes were noticeably different between MRI and EyePlan, with median DSC of 0.61 (IQR:0.21) and 0.74 (IQR:0.14) for RO1 and RO2 respectively. One radiation oncologist typically delineated smaller targets (Figure 3-a), with median volume ratios compared to EyePlan of 0.50 (IQR:0.32) and 0.74 (IQR:0.31) respectively. However, a good agreement was observed in tumor height ratio (HR) between the models. Also, agreement between the two observers improved for larger lesions (Spearman's rho = 0.57, p-value<0.01).

Independent of RO, tumor base area ratios had a significant impact on tumor volume ratio (Friedman's, p-value < 0.01), whereas tumor height ratios between models did not significantly affect volume discrepancies (Wilcoxon paired signed-rank test, p-value < 0.01). A strong positive correlation between area and volume ratios (AR-VR) was found (Spearman's rho = 0.84, p-value<0.01) (Figure 3-b).

The EyePlan model of the target volume showed high similarity in terms of clip-to-tumor distances, when compared with measurements performed by the ophthalmologist, with a median discrepancy of 0.20 mm (IQR: 0.20mm). Higher discrepancies were measured for tumors delineated on MRI with median differences of 2.00 mm (IQR: 2.11) and 1.20 mm (IQR:1.70 mm), for RO1 and RO2 respectively (Table 2).

Differences between EG_{EP} and EG_{MR} had no significant impact on target coverage. In contrast, planning on TV_{EP} or TV_{MR} resulted in significant variations of the dose distribution. Although acceptable coverage of TV_{MR} (V95=100%), when planned on TV_{EP} was achieved in 90% of cases, when planning on TV_{MR}, insufficient coverage on TV_{EP} was found in 90% and 58% of the cases for RO1 and RO2, respectively. Enlarging the safety margin by 1.5 mm could partially mitigate this, achieving clinically acceptable coverage of TV_{EP} in 87% and 71% of cases for RO1 and RO2 respectively.

DISCUSSION

The eye representation adopted in OPT consists of a geometrical eye and tumor model embedded in a dedicated treatment planning system. This study compares this model to one generated using patient specific delineation on MRI scans for a group of 33 OPT patients. It is indeed the presence of clips in both models that allowed for a rigorous geometrical comparison but since clips introduce artefacts on MRI images at the exterior surface of the eye globe, our study is partially limited by the fact that we did not have MRI for patients prior to clip implantation.

Compared to previous publications [3] [12], this analysis investigates differences observed between the two approaches for tumor volume definition not only for the overall volume, but also for their height and base (extension on the uvea) by evaluating their position with respect to clips implanted during surgery. Finally, a comprehensive analysis of the dosimetric implications of adopting a MRI based model has for the first time been performed.

Patients were able to actively maintain a stable gaze direction during the time of acquisition (~5 mins) and MRI images without relevant motion artefact were obtained. Ferreira et al used slightly shorter protocol and asked subjects to close the eyes during imaging and also reported limited motion artefact in the acquired images [18]. Of note, two (6%) patients presented with lesions that were invisible on MRI. In the first case, the tumor was flat and small, whilst in the second case, it was diffuse. Additionally, the presence of retinal detachment in both cases introduced uncertainty. The limited visibility of ocular lesions featuring this particular shape on MRI images has already been reported [12]. Nevertheless, MRI imaging of small lesions (thickness inferior to 2 mm) was achieved using higher magnetic fields (3 Tesla) [18]. The MRI imaging protocol used in this study however will not be sufficient for some patients presenting with diffuse/flat tumors with or without retinal detachment. On the other hand, the used MRI protocols did not exhibit clinically relevant geometrical distortions, with mean inter-clip distance discrepancies compared to the conventional method below 0.2 mm being observed. In addition, this demonstrates that despite appearing as a lack of signal in MRI images, clips can be recognized and delineated accurately.

Geometrically, a high similarity was measured when comparing the volumes of the eye globe modelled by EyePlan or delineated in MRI images, with volume ratios and DSCs of over 0.9. Nevertheless, it is reasonable to expect that MRI is better suited for an accurate representation of the eye globe and while the uncertainty in axial length determined by MRI is arguably higher compared to ultrasound measurement used by EyePlan, it is less dependent on the ability of the operator and less susceptible to artefacts due to ocular surgery.

On the other hand, significant discrepancies between the two models were observed in tumor volume definition however, with the TV_{MR} being, on average, smaller than TV_{EP} regardless of which radiation oncologist performed the contouring. Marnitz et al. presented similar results for such a comparison [3]. On the contrary, Daftari et al. have reported a significantly higher similarity in lesion volumes identified with conventional methods or MRI

[12], and a negligible variability between delineation performed by different observers. Similarly, we observed a decrease of delineation discrepancies between ROs as a function of tumor size suggesting that, the bigger the lesion, the more visible it is on MRI images. The introduction of automatic eye segmentation procedures for MRI images and the use of contrast agent could therefore make the segmentation more consistent [19] [20].

Our results demonstrate that, independent of observer, while the height of MRI-based tumor volume generally agrees with the ultrasound assessment used in the conventional approach, inconsistencies in the definition of the lesion base between the models produce the largest discrepancy in tumor volume definition. In EyePlan, the definition of the extent of the lesion on the retinal surface is based on defining tumor margins that best fit the measurement of clip-to-tumor distances performed at time of surgery (see Figure 4-b). During surgery, the ophthalmologist identifies the tumor base as the shadow the lesion casts on the eye surface under trans-illumination. Depending on the position of the light source and the shape of the tumor, its shadow would not precisely describe its base and arguably lead to overestimations. These surgical measurements are heavily dependent on the experience of the ophthalmologist performing the surgery and require interpretation. Ophthalmologists tend to be conservative when interpreting tumor borders also when the tumor base is defined in the EyePlan model as clips were, on average, more proximally located (0.2 mm) to the target than what was measured at times of surgery. Nevertheless, the clips on the sclera represent the main reference defining the tumor borders in an undoubtedly successful treatment protocol therefore the substantially increased difference of MR-based tumor bases to this reference cannot be ignored. In addition, results show that it is the definition of the tumor base that results in the largest discrepancies between observers delineating on MRI (mean area ratio of 1.36) in contrast to definition of the tumor height, where a good agreement has been found (mean height ratio 1.03). With the proposed protocol, even at the relatively high resolution achieved (0.5 mm), it is reasonable to expect that flat tumor basal extension could be missed on MRI scans. On the other hand, MRI is undoubtedly more suitable for defining accurately the shape and magnitude of the extent of an ocular melanoma into the vitreous body than the oversimplified geometrical model used in EyePlan (Figure 4-c) [21].

The dosimetric analysis confirmed that using MRI on its own for target delineation would introduce significant changes to the well-established and successful clinical standard employed nowadays. When applying plans generated on the MRI delineated targets, TV_{EP} was rarely covered in its entirety, an effect that could be only partially mitigated by a margin enlargement of 1.5mm. This demonstrates how the discrepancies in target volume definition between observers on MRI scans and with respect to EyePlan, especially in the basal extension of the tumor, are highly patient-specific and cannot be solved with a generalized solution. It is reasonable to expect that the geometrical reference provided by clips in combination with the integration of fundus imaging, even though in an oversimplified manner, makes EyePlan less susceptible to flat tumor extension misses (Figure 4-b). Thus, as proposed by Nurnberg et al. [8], it is our hypothesis that, the proposed 1.5 T MRI imaging protocol for uveal melanomas must be properly combined with higher resolution ophthalmological imaging such as fundus photography on a highly personalized and patient-specific basis. This multi-modal ocular imaging approach should be subjected to a thorough comparison to the current clinical standard and approved by ophthalmologists. Only then, considering the advantages that volumetric MRI imaging would bring to the overall accuracy of the eye model, an improved definition of the patient anatomy in ocular proton therapy will be achieved.

In conclusion, this study investigates the potential of 1.5 T MRI to define target volumes for ocular proton therapy. Compared to the current clinical standard, a generally good agreement was found for modelling the eye globe and target apex. However, using MRI

only there is a high risk to underestimate the base extent of the target volume. In addition, for particularly thin tumors, it was not possible to define the lesion using MRI, and there were substantial delineation discrepancies between observers. This however reduced as tumor size increased.

As such, although MRI has the potential to improve the accuracy of the eye model, on its own, it cannot replace the current clinical standard for target volume definition. While we acknowledge that the conservative approach applied in the current clinical standard may overestimate the target volume, adopting target volumes purely based on the proposed MRI protocol could negatively affect the high tumor control rates observed clinically using the standard approach. However, the situation could change with the introduction, in a geometrically accurate fashion, of complementary ophthalmological imaging into the MRI approach and with dedicated technical development in ocular MRI.

Bibliography

[1] J. Hrbacek, K. K. Mishra, A. Kacperek, R. Dendale, C. Nauraye, M. Auger, J. Herault, I. K. Daftari, A. V. Trofimov, H. A. Shih, Y.-L. E. Chen, A. Denker, J. Heufelder, T. Horwacik, J. Skavon, C. Hoehr, C. Duzenlu, A. Pica, F. Goudjil, A. Mazal, J. Thariat und D. C. Weber, «Practice Pattern Analysis of Ocular Proton Therapy Centers: The International OPTIC survey,» *International Journal of Radiation Oncology Biology Physics,* Bd. 95, Nr. 1, pp. 336-343, 2016.

[2] A. Kacperek, «Ocular Proton Therapy Centers,» in s *Ion Beam Therapy*, Berlin Heidelberg, Springer-Verlag, 2012, pp. 149-177.

[3] S. Marnitz, D. Cordini, R. Bendl, A. Lemke, J. Heufelder, I. Simiantonakis, H. Kluge, N. Bechrakis, M. Foerster und W. Hinkelbein, «Proton therapy of uveal melanomas,» *Strahlentherapie und Onkologie,* Bd. 182, Nr. 7, pp. 395-399, 2006.

[4] E. Egger, A. Schalenbourg, L. Zografos, L. Bercher, T. Boehringer, L. Chamot und G. Goitein, «Maximizing local tumor control and survival after proton beam radiotherapy of uveal melanoma,» *International Journal of Radiation Oncology Biology Physics,* Bd. 51, Nr. 1, pp. 138-47, 2001.

[5] E. Egger, L. Zografos, A. Schalenbourg und e. al, «Eye retention after protonbeam radiotherapy for uveal melanoma,» *Int J Radiat Oncol Biol Phys,* Bd. 55, pp. 867-880, 2003.

[6] M. Goitein und T. Miller, «Planning proton therapy of the eye,» *Med. Phys,* Bd. 10, Nr. 3, pp. 275-283, 1983.

[7] B. Dobler und R. Bendl, «Precise modelling of the eye for proton therapy of intra-ocular tumours,» *Physics in Medicine and Biology,* Bd. 47, Nr. 4, pp. 593-613, 2002.

[8] D. Nurnberg, A. Riechardt, O. Zeitz, J. Heufelder und A. Joussen, «Multimodal Imaging of the Choroidal Melanoma with DIfferential Diagnosis, Therapy, Radiation Planning and Follow-up,» *Kiln Monbl Augenheilkd,* Bd. 235, Nr. 9, pp. 1001-1012, 2018.

[9] K. Pfeiffer und R. Bendl, «Real-time dose calculation and visualization for the proton therapy of ocular tumours,» *Phys Med Biol,* Bd. 46, pp. 671-686, 2001.

[10] C. Rethfeldt, H. Fuchs und K. Gardey, «Dose distributions of a proton beam for eye tumor therapy: Hybrid pencil-beam and ray-tracing calculations,» *Med Phys,* Bd. 33, Nr. 3, pp. 782-791, 2006.

[11] R. Slopsema, M. Mamalui, J. Bolling, S. Flampouri, D. Yeung, Z. Li, M. Rutenberg und R. Dagan, «Can CT imaging improve targeting accuracy in clip-based proton therapy of ocular melanoma?,» *Phys. Med. Biol,* Bd. 64, p. 035010, 2019.

[12] I. K. Daftari, E. Aghaian, J. M. O'Brien, W. Dillon und T. L. Phillips, «3D MRI-based tumor delineation of ocular melanoma and its comparison with conventional techniques,» *Medical*

Physics, Bd. 32, Nr. 11, pp. 3355-3362, 2005.

[13] F. Hennings, A. Lomax, A. Pica, D. Weber und J. Hrbacek, «Automated treatment planning system for uveal melanomas treated with proton therapy: a proof fo concept analysis,» *International Journal of Radiation Oncology Biology Physics,* 2018.

[14] I. K. Daftari, K. K. Mishra, J. M. O'Brien, T. Tsai, S. S. Park, S. Martin und T. L. Phillips, «Fundus image fusion in EYEPLAN software: An evaluation of a novel technique for ocular melanoma radiation treatment planning,» *Medical Physics ,* Bd. 37, Nr. 10, pp. 5199-5207, 2010.

[15] I. Tsiapa, M. Tsilimbaris, E. Papdaki, P. Bouziotis, I. Pallikaris, A. Karantanas und T. Maris, «High resolution MR eye protocol optimization: Comparison between 3D-CISS, 3D-PSIF and 3D-VIBE sequences,» *Physica Medica,* Bd. 31, Nr. 7, pp. 774-780, 2015.

[16] E. Oberacker, K. Paul, T. Huelnhagen, C. Oezerdem, L. Winter, A. Pohlmann, L. Boehmert, O. Stachs, J. Heufelder, A. Weber, M. Rehak und I. Siebel, «Magnetic resonance safety and compatibility of tanatalum markers used in proton beam therapy for intraocular tumors: A 7.0 Tesla study,» *Magnetic Resonance in Medicine,* Bd. 78, p. 1553*1546, 2017.

[17] R. Via, F. Hennings, G. Fattori, A. Pica, A. Lomax, D. Weber, G. Baroni und J. Hrbacek, «Technical Note: Benchmarking automated eye tracking and human detection fro motion monitoring in ocular proton therapy,» *Medical Physics,* Bd. 47, Nr. 5, pp. 2237-2241, 2020.

[18] T. Ferreira, L. Fonk, M. Jaarsma-Coes, G. van Haren, M. Marinkovic und J. Beenaker, «MRI of uveal melanoma,» *Cancers,* Bd. 11, Nr. 377, 2019.

[19] C. Ciller, S. De Zanet, M. Ruegsegger, A. Pica, R. Sznitman, J. Thiran, P. Maeder, F. Munier und J. Kowal, «Automatic segmentation of the eye in 3D magnetic resonance imaging: A novel statistical shape model for treatment planning of retinoblastoma,» *International Journal of Radiation Oncology Biology Physics,* Bd. 92, Nr. 4, pp. 784-802, 2015.

[20] H.-G. Nguyen, R. Sznitman, P. Maeder, A. Schalenbourg, M. Peroni, J. Hrbacek, D. C. Weber, A. Pica und M. B. Cuadra, «Personalized anatomic eye model from T1-weighted VIBE Mr imaging of patients with uveal melanoma,» *Int J Radiat Oncol Biol Phys,* 2018.

[21] J. Beenakker, T. Ferreira, K. Soemarwoto, S. Genders, T. WM, A. Webb und G. Luyten, «Clinical evaluation of ultra-high-field MRI for three-dimensional visualization of tumour size in uveal melanoma patinets with direct relevance to treatment planning,» *Magn Reson Mater Phy,* Bd. 29, pp. 571-577, 2016.

Figure 1 On panel (a) and (b) the EG_{EP} and EG_{MR} for one patient are showed. On panel (c) a detail of tumor volumes as described using TV_{MR} (solid) and TV_{EP} (transparent) is presented after alignment based on clips position (grey dots in panel (a-b)). On panel (d) a schematic representation of the simplification adopted to estimate the tumor height considering tumor base area (TV_A) and the tumor volume.

Figure 2- A T1w-vibe and T2w-space MRI images of an exemplary uveal melanoma patient are shown on panel (a) and (b), respectively. The delineation of relevant eye structures (eye globe, lens tumour, highlighted with a white arrow and clip, highlighted with a black arrow) is visible on the images. On panel (c) the set-up for MRI acquisition: the surface loops coil is fixed on the examined eye and the reflection through the mirror placed in front of the patient's eye helps maintaining a stable gaze direction. Involuntary head movements are limited by the half-head coil, headphones and foam pads.

Figure 3 Geometrical comparison of target volume definition for the entire patient cohort. On the left panel, an orange and blue dots represent values of volume ratios and DSCs against the EyePlan model for delineation performed by radiation oncologist one (RO1) and two (RO2), respectively. The black dash line represents DSC values as a function of volume ratio corresponding to complete inclusion of the smaller volume into the larger one. Target volumes delineated by RO1 clustered towards smaller volume ratios values than the corresponding volumes for RO2. On panel (a), correlation plot for volume and area ratio between lesions delineated by RO1 (orange) and RO2 (blue) and the Eyeplan Model shows significant positive correlation between areas and volume definition.

Figure 4 Exemplary cases of difference in target volume definition between EyePlan (yellow contours) and MRI delineation performed by two radiation oncologists (RO1, orange contours, RO2, blue contours). On panel (a), a case

where good agreement between models was found. In panel (b), the tumor height is approximately the same for EyePlan and MRI but a considerable difference in the definition of the tumor base was found. It is appreciable how the tumor base defined in EyePlan extends to the clips position (dark region highlighted with white arrows). In panel (c), the simplified geometrical EyePlan model fails to accurately represent the tumor volume shape (region highlighted with dashed white arrow).
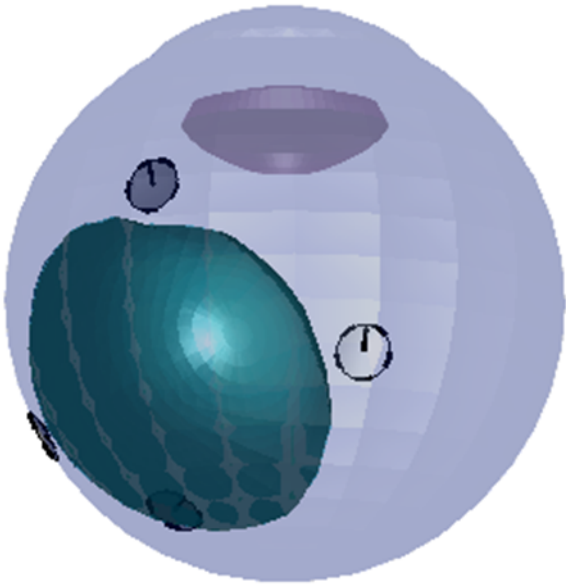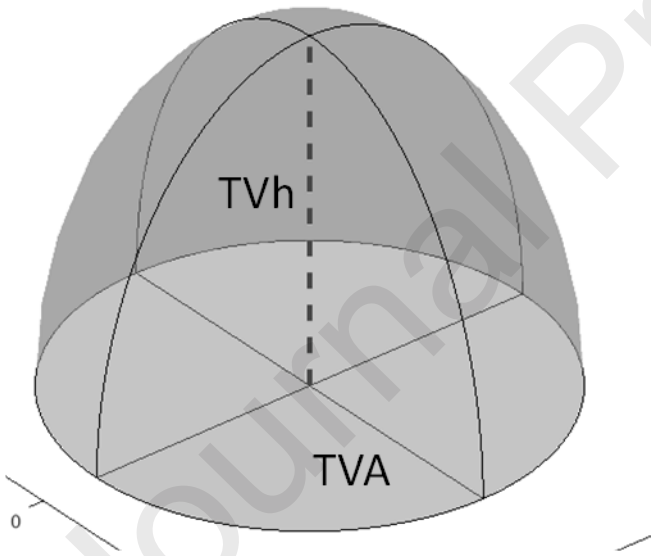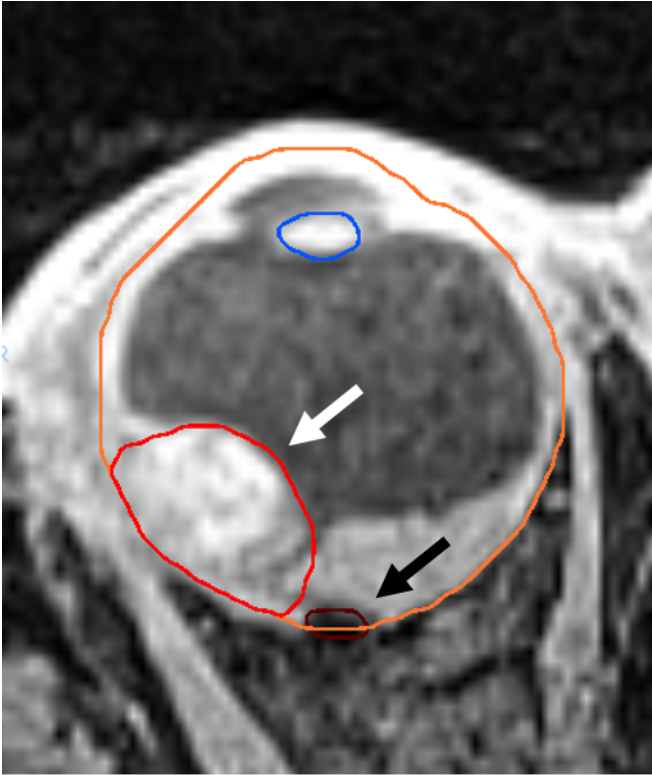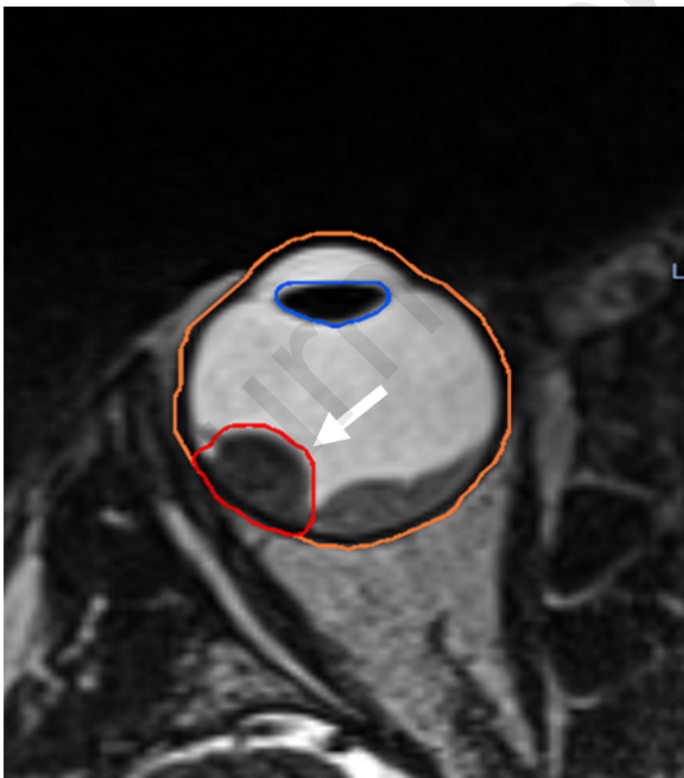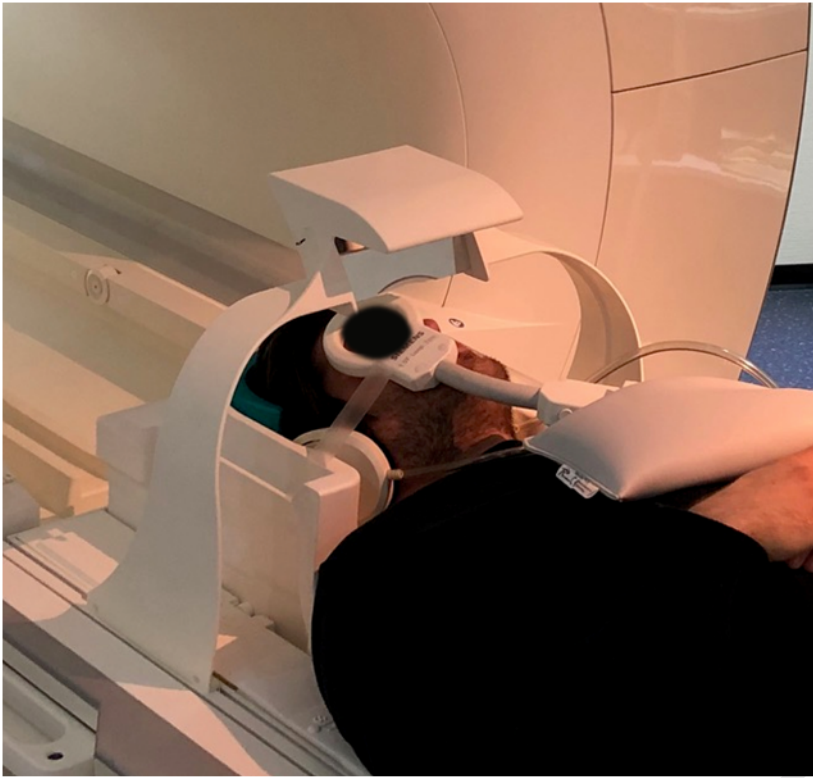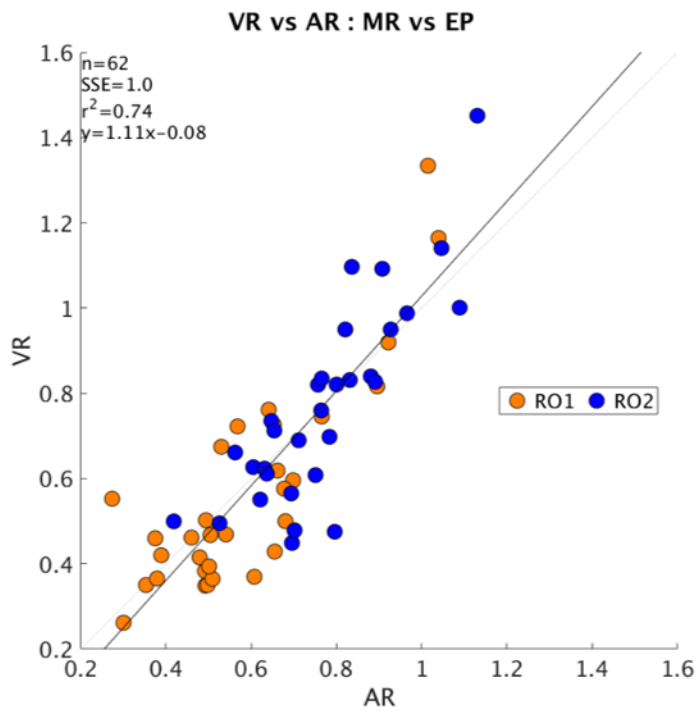

a)

b)
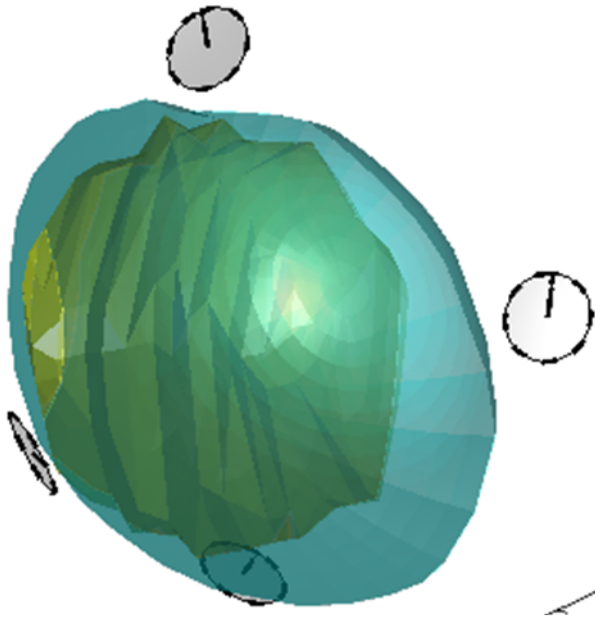
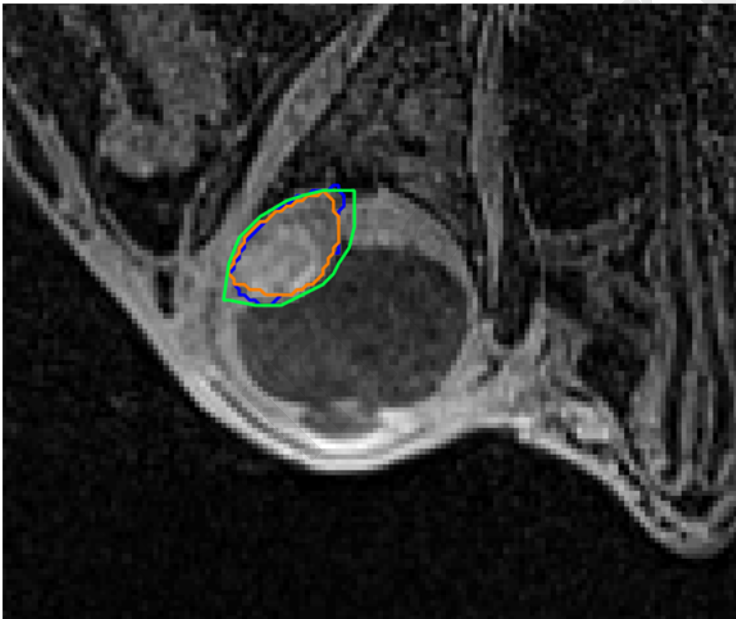c)

d)

a)

b)

c)
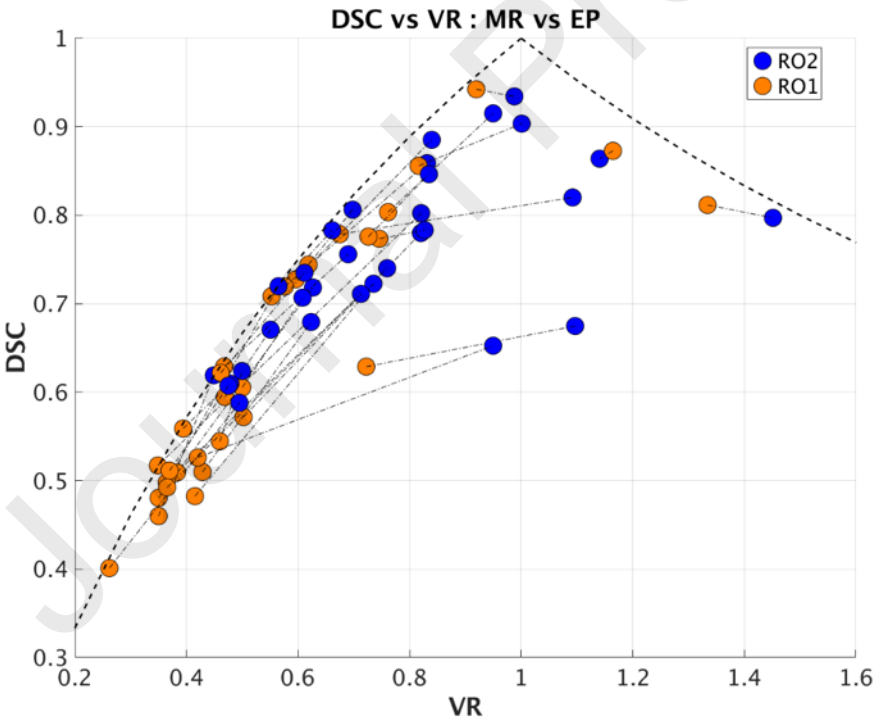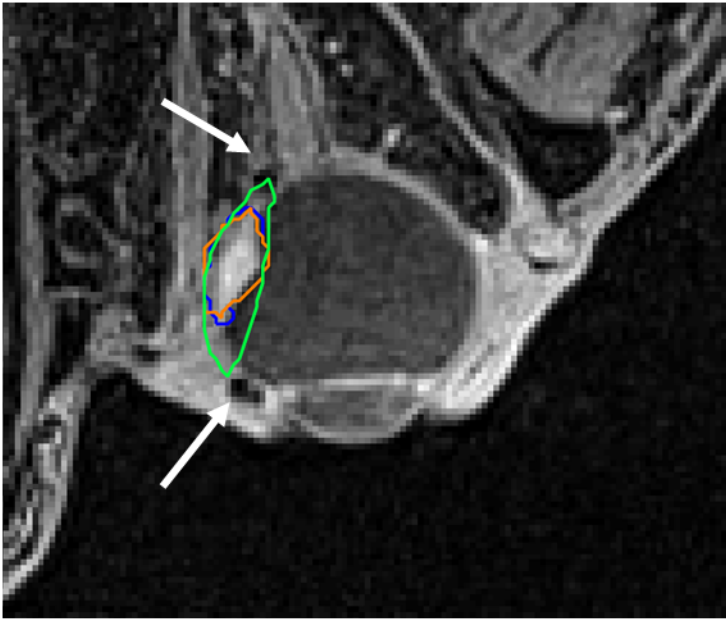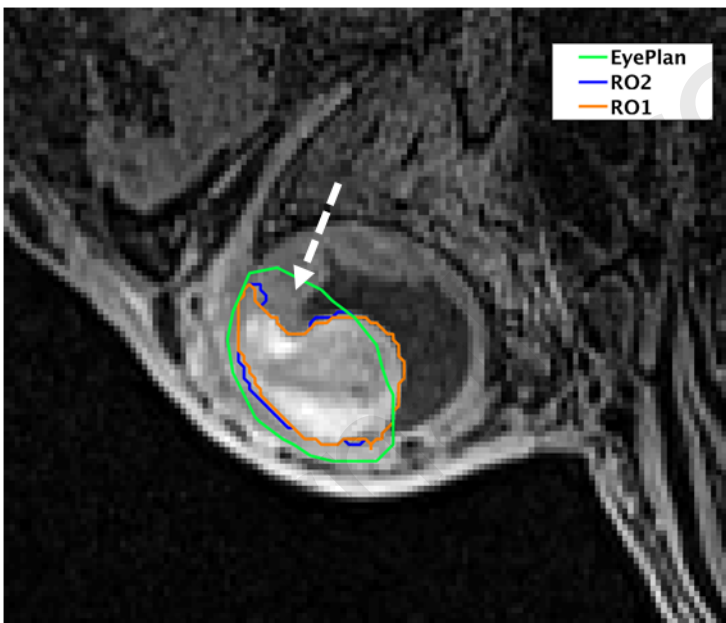

a)

b)

a)

b)

c)

Table 1 - Relevant information on the sequences' parameters used for T1-wiegthed and T2-weigthed volumetric MRI scans.

	T1w-VIBE	T2w-SPACE
TR/TE [ms]	6.55 / 2.39	1400 / 185
Flip angle [°]	12	150
Fat Suppression	SPAIR	-

Acquisition voxel size [mm]	0.5×0.5×0.5	0.5×0.5×0.5
Resolution	256x256x80	256x256x88
Parallel Imaging / Acceleration Factor	-	GRAPPA / 2
Distortion Correction	Enable	Enable
Image Post-processing (Filters)	Edge enhancement (3) Smoothing (3)	-
Total Scan Time [mm:ss]	04:17	05:01

Table 2 - Results of the geometrical comparison between target volume definitions in Eyeplan and through MRI delineation. For the tumor volume distances to clips, the table reports the discrepancies between all three models and the measurement performed during surgery.

Organ	Index		Median	IQR
Eye Globe	VR		0.97	0.12
	DSC		0.92	0.03
Lens	VR		1.41	0.32
	DSC		0.68	0.19
Tumor	VR	RO1	0.47	0.32
		RO2	0.74	0.31
	DSC	RO1	0.61	0.26
		RO2	0.74	0.14
	AR	RO1	0.53	0.19
		RO2	0.76	0.22
	HR	RO1	0.99	0.17
		RO2	0.93	0.30
	Distance to clip [mm]	RO1	2.00	2.11
		RO2	1.20	1.70
		EP	0.20	0.20
Intra-observer difference (RO1 vs RO2)				
Tumor	VR		1.32	0.45
	DSC		0.63	0.26
	AR		1.36	0.38
	HR		1.03	0.15

VR: volume ratio; DSC: Dice Similarity Coefficient; AR: Area Ratio, HR: Height Ratio; RO1: Radiation Oncologist 1; RO2: Radiation Oncologist 2; EP: EyePlan

- The potential and pitfalls of target volume definition in ocular proton therapy based on Magnetic Resonance Imaging (MRI) were investigated and compared to the conventional clinical method based on metallic clips implantation on 33 uveal melanoma patients.
- In contrast to previous publications, an extensive description of discrepancies between the different modelling of the target volumes, together with a thorough investigation of the causes, is performed, as well as an investigation into the potential dosimetric consequences.
- For two out of thirty-three (6%) patients the lesion was invisible in MRI. Significant discrepancies between MRI and clips-based eye models were observed for tumor volume definition in the remaining dataset, with the MRI volumes being, on average, smaller than the clips-based one. Our results demonstrate that, independent of observer, while the height of MR-based tumor volume agrees with the ultrasound assessment used in the conventional approach, inconsistencies in the definition of the base of the tumour between the models produce the largest discrepancy in tumor volume definition.
- We observed a decrease of delineation discrepancies between radiation oncologists as a function of tumor size suggesting that, the bigger the lesion, the more visible it is on MRI images
- Although the proposed MRI protocol has the potential to improve the accuracy of the eye model, on its own, it cannot replace the current clinical standard for target volume definition. However, the situation could change with the introduction of complementary ophthalmological imaging into the MRI approach in a geometrically accurate fashion.